NASA TECHNICAL MEMORANDUM

NASA TM X-72715

NASA TM X-72715

WIND TUNNEL/FLIGHT DATA CORRELATION FOR THE BOEING 737-100 TRANSPORT AIRPLANE

BY FRANCIS J. CAPONE

AUGUST 1975

(NASA-TM-X-72715) WIND TUNNEL/FLIGHT DATA CORRELATION FOR THE BOEING 737-100 TRANSPORT AIRPLANE (NASA) 18 p HC $3.25 CSCL 01C

N75-31051

Unclas
G3/05 35262

This informal documentation medium is used to provide accelerated or special release of technical information to selected users. The contents may not meet NASA formal editing and publication standards, may be revised, or may be incorporated in another publication.

NATIONAL AERONAUTICS AND SPACE ADMINISTRATION
LANGLEY RESEARCH CENTER, HAMPTON, VIRGINIA 23665

1. Report No.	2. Government Accession No.	3. Recipient's Catalog No.
NASA TM X-72715		
4. Title and Subtitle Wind Tunnel/Flight Data Correlation for the Boeing 737-100 Transport Airplane		5. Report Date August 1975
		6. Performing Organization Code
7. Author(s) Francis J. Capone		8. Performing Organization Report No.
9. Performing Organization Name and Address NASA Langley Research Center Hampton, Virginia 23665		10. Work Unit No. 505-04-11-01
		11. Contract or Grant No.
12. Sponsoring Agency Name and Address National Aeronautics and Space Administration Washington, DC 20546		13. Type of Report and Period Covered Technical Memorandum
		14. Sponsoring Agency Code

15. Supplementary Notes

Special Technical Information Release, not planned for formal NASA publication

16. Abstract

A brief wind-tunnel/flight data correlation for the Boeing 737-100 airplane has been made. The wind-tunnel data were published in NASA TN D-5971. The results showed excellent agreement between wind-tunnel and flight trimmed drag polars at Mach numbers less than 0.67. The wind-tunnel data predicted larger drag increments due to compressibility and a lift-curve slope about 9 percent higher than flight.

17. Key Words (Suggested by Author(s)) (STAR category underlined)	18. Distribution Statement
Aerodynamics Subsonic Transport Wind Tunnel Data Flight Data	Unclassified Unlimited

19. Security Classif. (of this report)	20. Security Classif. (of this page)	21. No. of Pages	22. Price*
Unclassified	Unclassified	17	$3.25

*Available from { The National Technical Information Service, Springfield, Virginia 22161
STIF/NASA Scientific and Technical Information Facility, P.O. Box 33, College Park, MD 20740

SUMMARY

A brief wind-tunnel/flight data correlation for the Boeing 737-100 airplane has been made. The wind-tunnel data were published in NASA TN D-5971. The results showed excellent agreement between wind-tunnel and flight trimmed drag polars at Mach numbers less than 0.67. The wind-tunnel data predicted larger drag increments due to compressibility and a lift-curve slope about 9 percent higher than flight.

INTRODUCTION

The National Aeronautics and Space Administration and the Boeing Company conducted a cooperative wind-tunnel/flight data correlation program for the Boeing 737-100 transport airplane during January 1968. The 737 airplane is a twin-turbofan, short-haul, subsonic transport capable of carrying about 100 passengers. The results of the wind-tunnel study conducted in the Langley 16-foot transonic tunnel are presented in reference 1. A correlation of this wind-tunnel data with the flight data supplied at that time by the Boeing Company was made but not published because an adequate analysis to account for the known differences between the airplane and wind-tunnel model was not made. In 1973, the Langley Research Center purchased a Boeing 737-100 airplane in order to conduct a variety of flight research programs including wind tunnel/flight correlations. Because of this recent acquisition, it now becomes appropriate to document the brief wind-tunnel/flight data correlation mentioned above.

SYMBOLS

Model forces and moments were referred to a stability axis system with the model moment reference center located 82.80 centimeters rearward of the model nose corresponding to 22.4 percent of the wing mean aerodynamic chord which was approximately at the nominal center-of-gravity position of the airplane.

A	aspect ratio
A_w	wetted area
b	span
$\bar{c}$	wing mean aerodynamic chord
C_D	drag coefficient, $\frac{Drag}{qS}$
$(C_{D,f})_F$	computed flight skin-friction drag coefficient
$(C_{D,f})_{F,av}$	average computed flight skin-friction drag coefficient
$(C_{D,f})_{W.T.}$	computed wind-tunnel skin-friction drag coefficient
$C_{D,trim}$	trim drag coefficient
C_L	lift coefficient, $\frac{Lift}{qS}$
$C_{L,trim}$	trim lift coefficient
C_{L_α}	lift-curve slope per degree
$\Delta C_{D,f}$	$(C_{D,f})_{W.T.} - (C_{D,f})_{F,av}$

$\Delta C_{D,M}$	drag-coefficient increment due to compressibility $[C_D]_M - [C_D]_{M = 0.55}$
H	altitude
ℓ_{ref}	reference length
M	free-stream Mach number
M_{av}	average free-stream Mach number
p_∞	free-stream static pressure
q	free-stream dynamic pressure
R	Reynolds number based on $\bar{c}$
R_{av}	average Reynolds number
R_N	Reynolds number per meter
S	wing reference area
T_t	stagnation temperature
W	airplane mass
δ	static-pressure correction parameter for correction to standard sea-level conditions (p_∞/101325)
δ_h	incidence angle of horizontal tail, positive when trailing edge is down

MODEL AND AIRPLANE

A sketch of the 737 airplane is shown in figure 1. The airplane is a twin-turbofan, short-haul, subsonic transport weighing about 45000 kilograms, capable of carrying about 100 passengers at a cruise Mach number between 0.78 and 0.80.

Complete details of the 0.062-scale model can be found in reference 1. The model-component designation of reference 1 will also be used and, for this correlation, data for configuration $BW_1 HVN_1 T$ will be presented. Photographs of the wind-tunnel model are given in figure 2.

The following known differences existed between the model and airplane. The airplane had open landing gear wells, that is, there were no panels covering the landing gear. The model fuselage was constructed with a smooth underside and no attempt was made to simulate the open landing well with the gear in it. An auxiliary power unit exhaust located at the end of the airplane fuselage was not simulated. For the wind-tunnel model, the nacelle inlet velocity ratio was matched to the airplane. As a result, the model nacelle exit area was larger than the equivalent scaled airplane nozzle exit area. Because of this difference in nacelle exit area, the model nacelle afterbody boattail angle was 7° whereas the airplane boattail angle was 10.9°. No allowance was made on the wind-tunnel model for wing twist due to aeroelastic effects. The wing twist under flight conditions was estimated by Boeing to be 1 to 1.5°.

ADJUSTMENTS TO DATA

The wind-tunnel data of reference 1 have been adjusted for nacelle internal axial force and support interference effects. No other adjustments were made to these data. The wind-tunnel trimmed drag polars from reference 1, (figure 17 (d)) are presented herein as figure 3.

Flight test results were supplied by the Boeing Company. These flight data as supplied were reduced with a reference area of $0.349 m^2$ model scale. These results were then adjusted to the wind tunnel reference area of $0.367 m^2$. A trailing cone was used to determine airplane Mach number. A drag coefficient of 0.0003 (measured with "fish scale" type balance) was subtracted from the flight drag coefficients to account for the drag of the trailing cone. These drag coefficients along with other pertinent flight measurements and conditions are presented in Table I.

Skin-friction drag coefficients were computed at wind tunnel and flight conditions using the method of reference 2. Information required for these computations are presented in Tables I to III. The flight drag coefficients have been adjusted to the average skin-friction drag coefficient (Table I) and are also presented in Table I, and in figure 4 (identified with symbols). Average flight skin-friction drag coefficients (Table I) were plotted versus Mach number and values of $(C_{D,f})_{F,av}$ were read off the plot at the Mach numbers at which wind tunnel data were obtained. The difference between the wind tunnel skin-friction drag coefficient and these values was then subtracted from the wind-tunnel drag polars. This incremental skin-friction drag coefficient is also presented in Table III.

An adjustment is made to the skin-friction drag coefficients to account for thickness effects (ref. 3) using a form factor of 1.18 for the entire configuration (ref. 1). This adjustment increases the $\Delta C_{D,f}$ increments of Table III by 0.0009. A value for excrescence or roughness drag coefficient (ref. 3) of 0.0018 was obtained from the Boeing Company and has also been added to the trimmed wind-tunnel drag polars. These final adjusted trimmed wind-tunnel drag polars (adjusted for skin-friction, thickness and roughness effects) are presented in figure 4 by the dashed lines.

SUMMARY OF RESULTS

Comparisons of adjusted wind tunnel and adjusted flight drag polars are presented in figure 4. There is excellent agreement at M = 0.596 and 0.672. However, there are larger differences between the adjusted wind-tunnel and flight drag polars at the higher Mach numbers.

A comparison of flight and wind-tunnel compressibility drag rise characteristics is presented in figure 5. The wind-tunnel data shows the drag rise to occur earlier than the flight data and also predicts larger drag increments due to compressibility effects.

A comparison of flight and wind-tunnel (figure 17(a), ref. 1) lift-curve slopes is given in figure 6. The wind-tunnel lift-curve slopes are about 9 percent higher than flight determined values.

REFERENCES

1. Capone, Francis J.: Longitudinal Aerodynamic Characteristics of a Twin-Turbofan Subsonic Transport With Nacelles Mounted Under the Wings. NASA TN D-5971, 1970.

2. Sommer, Simon C.; and Short, Barbara J.: Free-Flight Measurements of Turbulent-Boundary-Layer Skin Friction in the Presence of Severe Aerodynamic Heating at Mach Numbers From 2.8 to 7.0. NACA TN-3391, 1955.

3. Brown, Clinton E.; and Chen, Chuan Fang: An Analysis of Performance Estimation Methods for Aircraft. NASA CR-921, 1967.

TABLE I. - TABULATED FLIGHT DATA

Symbol	M	M_{av}	H,m	R_N x 10^{-6}	C_L	C_D	$(C_{D,f})_F$	$(C_{D,f})_{F,av}$	Adjusted C_D	W kg. x 10^{-3}	W/δ x 10^{-3}	Ave.C.G. in % mac
○	0.594	0.596	8458	6.01	0.464	0.0281	.0130	.0127	.0278	37.19	113.4	21.8
○	.597		7272	6.86	.365	.0247	.0128		.0246	35.02	89.8	22.9
○	.599		5761	8.05	.275	.0221	.0125		.0223	32.84	68.0	21.6
○	.595		2785	10.72	.185	.0202	.0120		.0209	32.11	45.4	22.3
○	.595		9246	5.46	.550	.0315	.0132		.0310	38.78	134.7	22.5
□	0.678	0.672	3427	6.89	0.357	0.0247	.0126	.0124	.0245	37.47	113.4	21.8
□	.663		10128	5.57	.516	.0302	.0131		.0297	40.14	156.9	23.0
□	.677		9278	6.26	.427	.0267	.0128		.0263	39.33	135.2	23.2
□	.671		6883	8.04	.290	.0226	.0124		.0226	37.19	90.3	21.7
□	.672		5347	9.42	.217	.0208	.0121		.0210	34.43	67.6	23.0
□	.674		2842	12.08	.144	.0198	.0117		.0205	31.93	45.4	22.1
◇	0.738	0.736	10045	6.26	0.420	0.0284	.0127	.0124	.0281	41.10	158.8	23.2
◇	.731		9387	6.68	.371	.0258	.0126		.0256	39.33	137.4	[illegible]
◇	.740		8288	7.63	.298	.0232	.0124		.0232	38.06	112.9	[illegible]
◇	.736		7230	8.50	.241	.0217	.0122		.0219	35.42	90.3	[illegible]
◇	[illegible]		10903	5.61	.490	.0310	.0130		.0304	40.91	180.5	[illegible]
◇	.743		8185	7.75	.292	.0236	.0123		.0237	38.19	111.6	22.0
◇	[illegible]		5240	10.43	.181	.0208	.0118		.0214	34.93	67.6	22.8
△	[illegible]	0.750	10837	5.86	0.456	0.0324	.0128	.0124	.0320	41.23	180.5	22.2
△	[illegible]		10121	6.28	.410	.0285	.0127		.0282	[illegible]	[illegible]	22.8
△	[illegible]		[illegible]	[illegible]	[illegible]	.0254	.0125		.0253	[illegible]	[illegible]	23.5
△	[illegible]		[illegible]	9.09	[illegible]	[illegible]	.0120		.0224	[illegible]	[illegible]	[illegible]
△	[illegible]		[illegible]	[illegible]	[illegible]	[illegible]	.0118		.0214	[illegible]	[illegible]	[illegible]

TABLE I. - TABULATED FLIGHT DATA (CONT'D)

Symbol	M	M_{av}	H,m	R_N x 10^{-6}	C_L	C_D	$(C_{D,f})_F$	$(C_{D,f})_{F,av}$	Adjusted C_D	W kg. x 10^{-3}	W/δ x 10^{-3}	Ave.C.G. in % mac
△	0.777	0.774	10000	6.63	0.381	0.0297	.0126	.0122	.0293	41.55	159.2	22.8
△	.776		9237	7.21	.328	.0267	.0124		.0265	39.87	136.1	23.5
△	.773		8198	8.05	.272	.0244	.0122		.0244	38.42	112.5	22.0
△	.773		7082	9.07	.216	.0221	.0120		.0223	35.70	88.9	22.4
△	.770		4950	11.24	.165	.0212	.0116		.0218	35.38	67.6	21.9
D	0.801	0.800	9116	7.54	0.306	0.0294	.0123	.0121	.0292	40.50	135.6	23.6
D	.801		8204	8.34	.256	.0270	.0122		.0269	38.83	113.8	22.3
D	.798		6983	9.46	.204	.0243	.0119		.0245	36.47	89.8	22.0
	0.421		5412	5.86	0.550	0.0320	.0132			34.11	57.6	23.3
	.495		5838	6.60	.404	.0257	.0129			32.57	68.5	22.0
	.788		9948	6.76	.370	.0315	.0125			41.87	159.2	22.6

TABLE II. - REFERENCE DIMENSIONS, WETTED AREAS AND REFERENCE LENGTHS

(a) Reference dimensions

	Model	Airplane
S, m^2	0.367	95.58
$\bar{c}$, m	.211	3.41
b, m	1.760	28.39
A	8.410	8.41

(b) Wetted areas and reference lengths

Component	Model		Airplane	
	A_w, m^2	ℓ_{ref} m	A_w m^2	ℓ_{ref} m
Fuselage and wing-root flap track fairing	1.026	1.712	266.81	27.61
Wing	.573	.195	149.10	3.14
Horizontal tails	.182	.143	47.29	2.31
Vertical tail	.165	.217	42.92	3.49
Pylons	.021	.344	5.57	5.55
Nacelles	.148	.345	38.46	5.57
Outboard flap track fairings	.026	.176	6.69	2.84

TABLE III. - WIND TUNNEL AND FLIGHT REYNOLDS NUMBER AND SKIN FRICTION COEFFICIENTS; INCREMENTAL SKIN FRICTION

	Wind Tunnel			Flight		
M	T_t, °K	R x 10^{-6}	$(C_{D,f})_{W.T.}$	R_{av} X 10^6	$(C_{D,f})_{F,av}$	$\Delta C_{D,f}$
0.550	301	2.248	0.0179			.0048
.596				25.30	0.0127	
.625	307	2.403	.0175			.0049
.672				27.43	.0124	
.725	315	2.528	.0172			.0048
.736				25.75	.0124	
.750	323	2.568	.0171	26.58	.0124	.0047
.774				28.78	.0122	
.775	322	2.593	.0170			.0048
.800	316	2.625	.0170	28.80	.0121	.0049
.825	328	2.646	.0169			
.850	325	2.701	.0168			

R based on wing $\bar{c}$

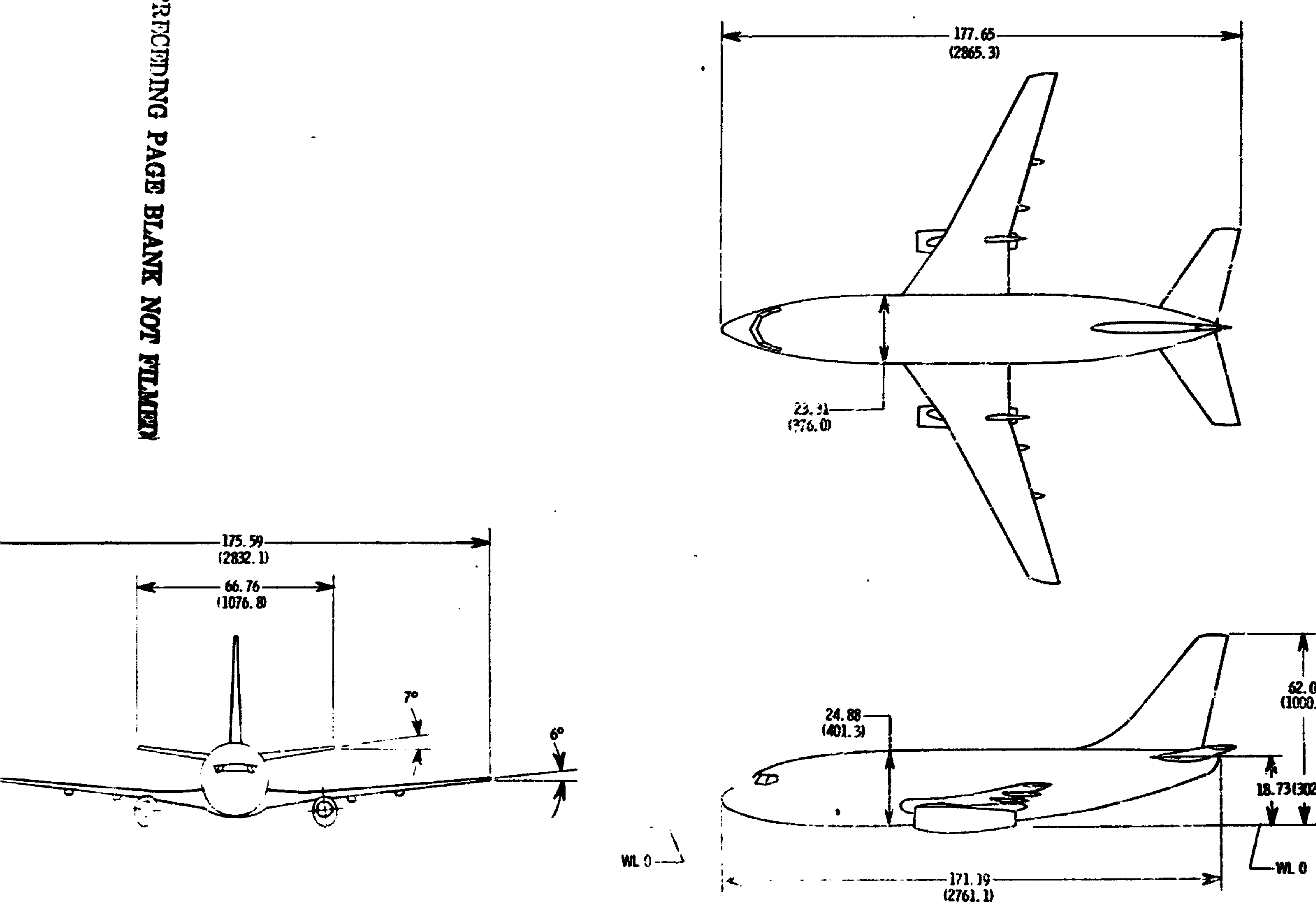

Figure 1. - Sketch of transport. Parenthetical dimensions are for full scale airplane. All dimensions are in centimeters unless otherwise noted.

NASA

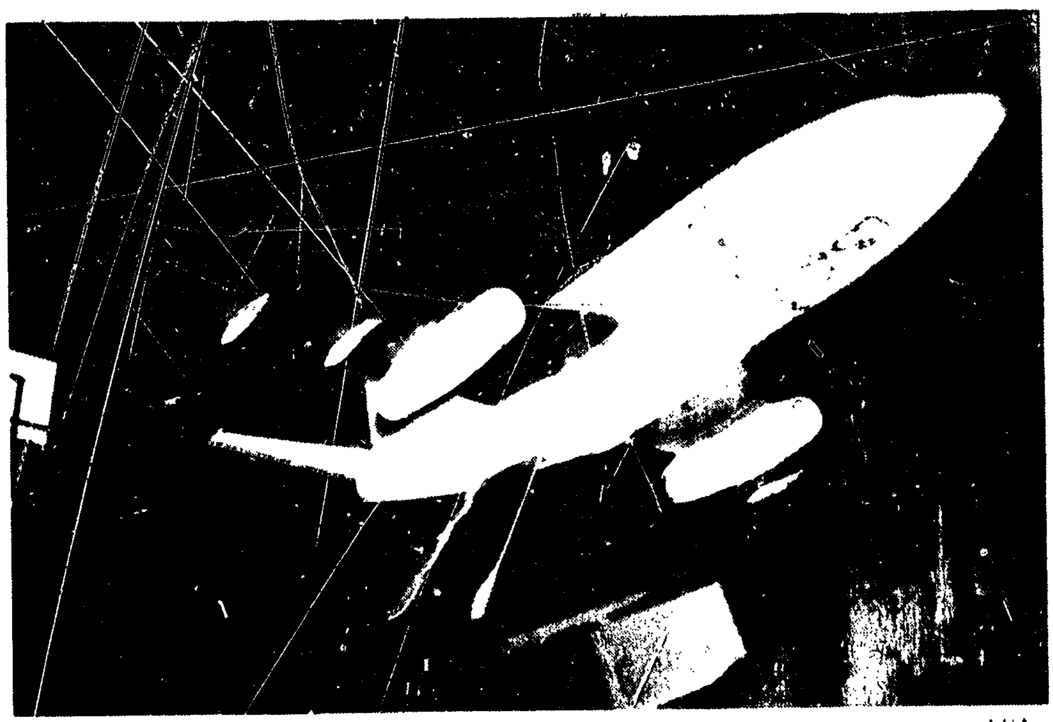

NASA

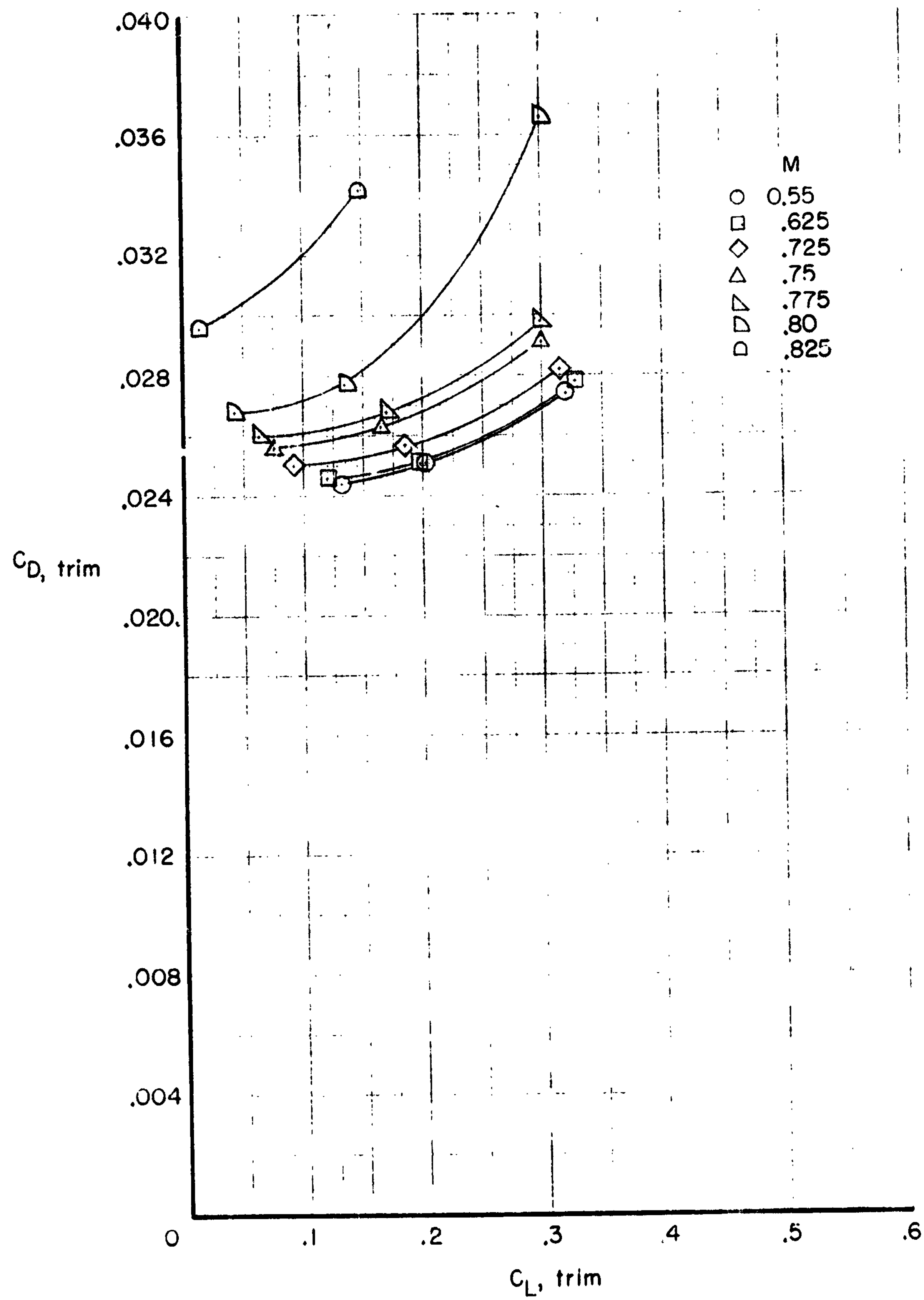

Figure 3. - Wind tunnel trimmed drag polars. Symbols represent trim points.

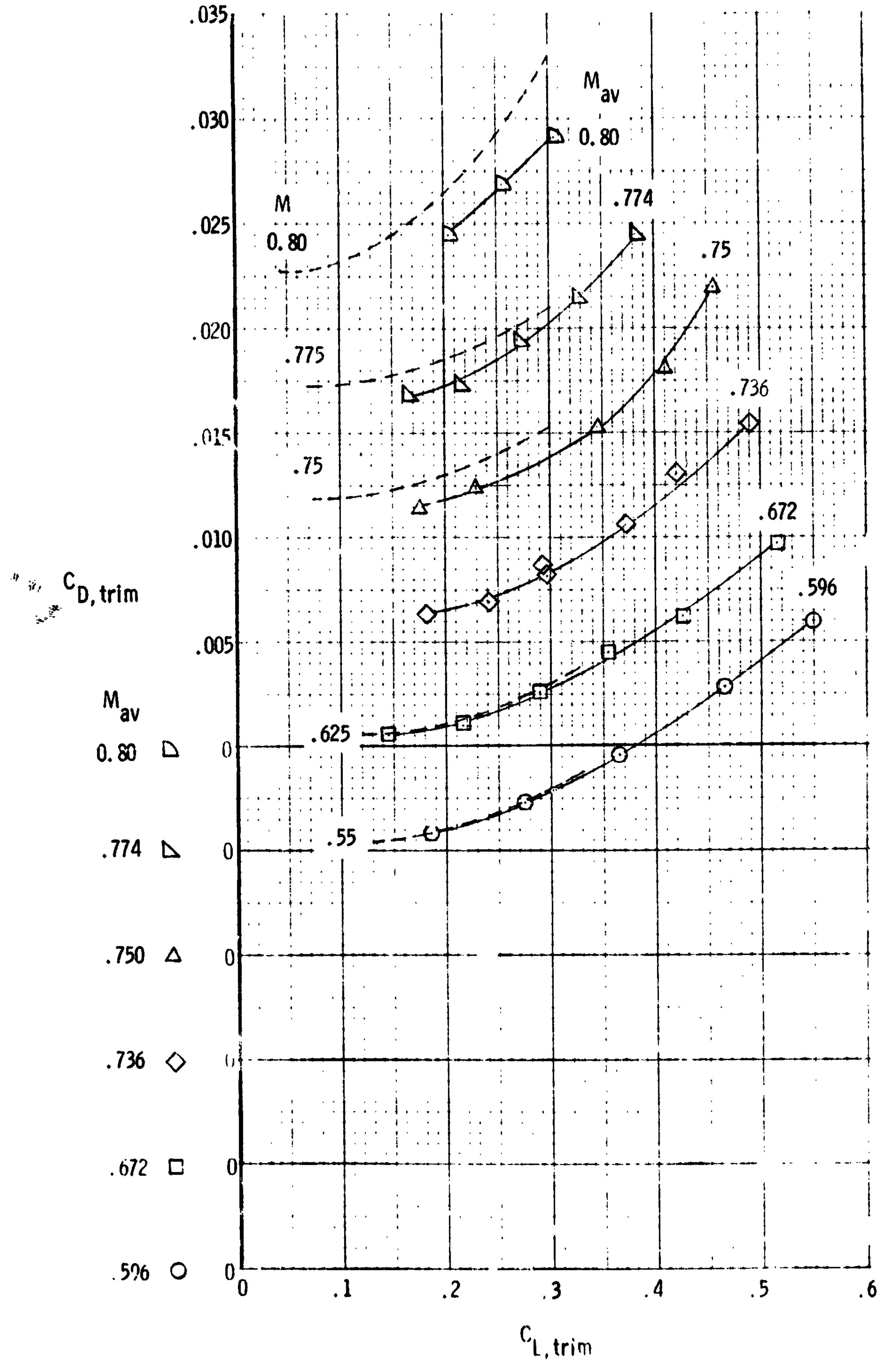

Figure 4. - Comparison of flight and wind-tunnel trimmed drag polars. Symbols represent adjusted flight data.

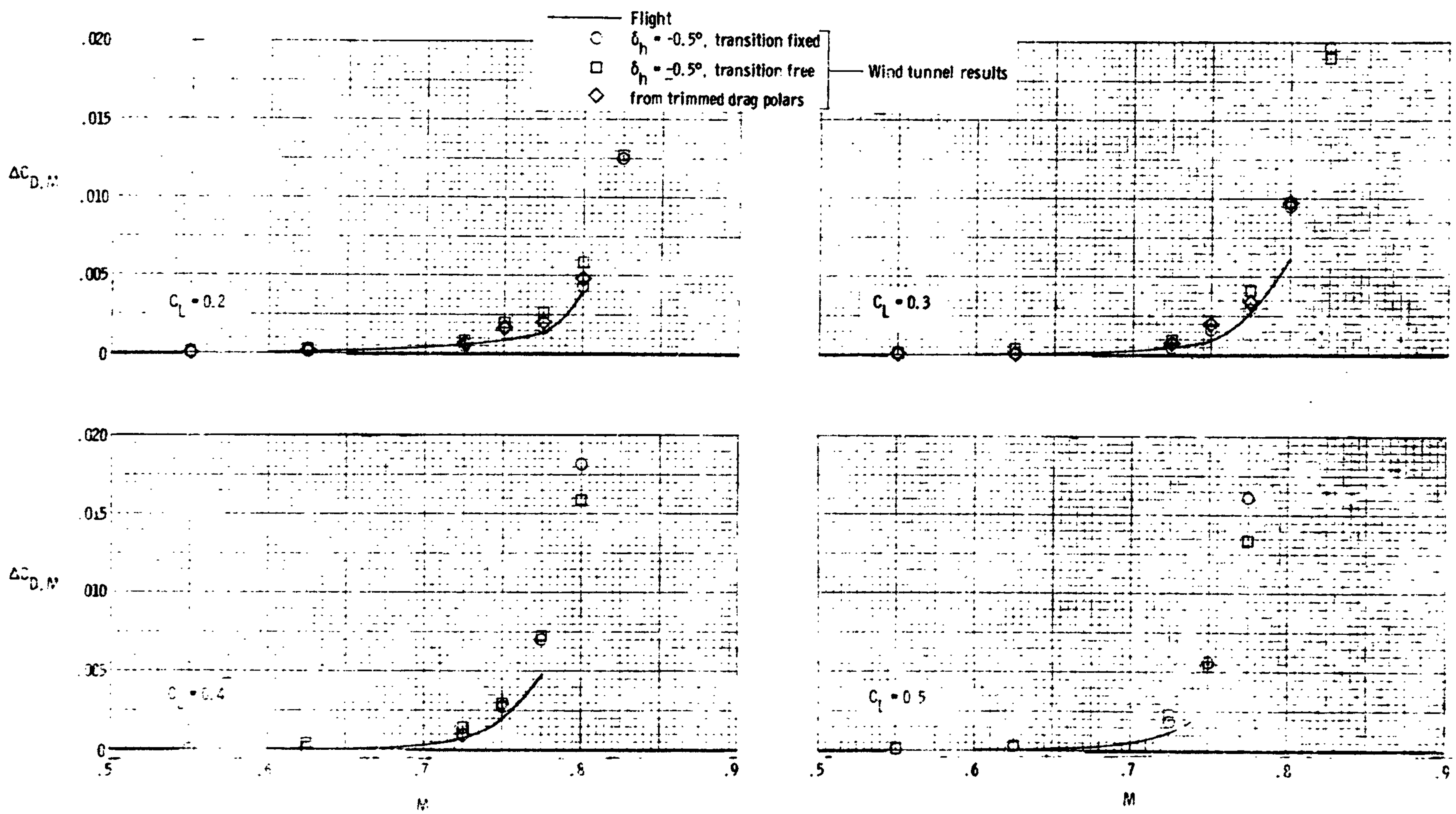

Figure 5. - Comparison of flight and wind tunnel compressibility drag rise characteristics.

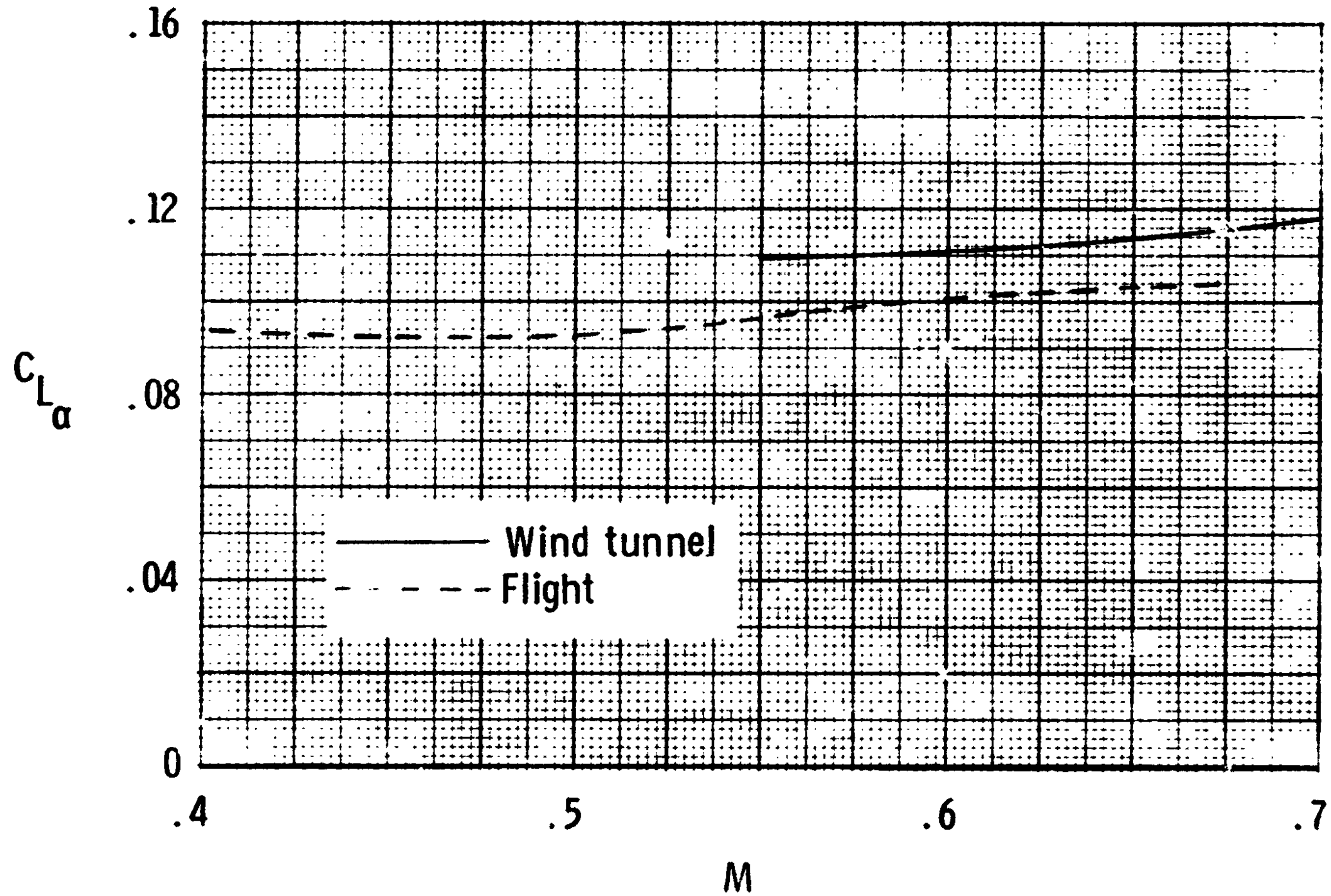

Figure 6. - Comparison of lift curve slopes.